



SHORT REPORT

Fine mapping of a distinctive autosomal dominant vacuolar neuromyopathy using 11 novel microsatellite markers from chromosome band 19p13.3

F Sangiuolo¹, E Bruscia¹, F Capon¹, S Servidei², B Dallapiccola³ and G Novelli¹

¹Dipartimento di Biopatologia e Diagnostica per Immagini, Sezione di Genetica, Università Tor Vergata; ²Istituto di Neurologia, Università Cattolica del Sacro Cuore; ³Dipartimento di Medicina Sperimentale e Patologia, Università di Roma La Sapienza e Istituto CSS Mendel, Rome, Italy

We previously mapped a distinctive autosomal dominant vacuolar neuromyopathy on human chromosome 19p13 in an 8cM region, delimited by D19S209 and D19S177 markers. We now report the fine mapping of the disease locus within an interval of 250 Kb by haplotype analysis performed using a set of 11 novel microsatellite markers isolated from the candidate region. *European Journal of Human Genetics* (2000) 8, 809–812.

Keywords: vacuolar neuromyopathy; chromosome 19; linkage; microsatellite markers

Introduction

We previously reported a large Italian family affected by a distinctive autosomal dominant vacuolar neuromyopathy (OMIM 601846), characterised by a generalised muscle weakness and atrophy with distal-to-proximal progression sparing facial and ocular muscles, dysphonia and dysphagia, pes cavus and areflexia, variable clinical expression ranging from subclinical myopathy to severely disabling weakness, and mixed neurogenic and myopathic abnormalities on electromyography.¹ A genome-wide scan mapped the disease to the short arm of chromosome 19, within an 8cM interval between D19S209 and D19S177 markers.¹ We report the refinement of the disease-locus mapping to a 250 Kb interval by extensive haplotype analysis using a set of 11 novel microsatellite markers isolated from the critical region.

Materials and methods

Microsatellite analysis

Primers flanking nucleotide repeats were designed from publicly available cosmid sequences (<http://www-bio.llnl.gov/>) spanning the area of interest (Table 1). All markers were amplified from genomic DNA using [³²P] dCTP, at the annealing temperatures reported in Table 1. Primer sequences

are available at <http://srs.ebi.ac.uk/>. Accession numbers are given in Table 1. Amplified products were separated on denaturing polyacrylamide gels, using a M13 sequence for allele sizing. A sample of 50 unrelated individuals was genotyped at all loci, in order to determine allele frequencies and heterozygosity values for each marker.

Linkage analysis

We genotyped the 11 novel markers in all family members, including affected subject IV-4 whose DNA was not available at the time of our genome-wide scan (Figure 1A). Two-point lod scores were calculated at each locus using the MLINK program from the LINKAGE package.² Haplotypes were derived by minimizing recombination events and were also confirmed using the 'haplotype on' function of GENE-HUNTER + program.³ The *tel-cen* order and the inter-marker distances used for haplotype construction were inferred from the Lawrence Livermore chromosome 19 cosmid map (available at <http://www-bio.llnl.gov/>).

Results and discussion

Eleven novel polymorphic markers were characterised with respect to allele frequencies and heterozygosity (Table 1). All the analysed repeats proved to be polymorphic; in particular, the (TGAA) repeat on 27139 cosmid and the (CA) repeat on 335474 cosmid showed the highest heterozygosity values (0.97 and 0.83, respectively). Locus order and distances between markers are determined, based on sequence data from the Lawrence Livermore chromosome 19 cosmid map.

Correspondence: Giuseppe Novelli PhD, Dipartimento di Biopatologia e Diagnostica Per Immagini, Sezione di Genetica, Ed. E Nord p.t., Facoltà di Medicina e Chirurgia, Università Tor Vergata, via di Tor Vergata 135 00133 Roma, Italy. Tel: + 39 06 72596078; Fax: + 39 06 20427313; E-mail: novelli@med.uniroma2.it

Received 22 April 2000; revised 21 June 2000; accepted 29 June 2000

Table 1 Microsatellite marker polymorphisms on 19p13.3

Cosmid (LLNL acc. no.)	Repeat	Observed het (%) ^a	Allele size (frequency)	Annealing temp, deg C	Marker accession number
R27139 (LLNL-R 231E11)	TGAA	97	141 (0.16); 145 (0.05); 153 (0.47); 157 (0.33)	58	AJ277262
R27139 (LLNL-R 231E11)	TG	56	317 (0.04); 319 (0.5); 321 (0.36); 323 (0.1)	55	AJ277263
R26529 (LLNL-R 225C1)	TA	57	178 (0.07); 184 (0.37); 186 (0.22); 190 (0.11); 194 (0.07); 204 (0.15); 208 (0.02)	58	AJ277264
R30140 (LLNL-R 262G12)	GT	57	79 (0.03); 81 (0.67); 83 (0.21); 85 (0.07)	53	AJ277254
R28154 (LLNL-R 242B6)	ATT	68	224 (0.34); 227 (0.09); 230 (0.25); 233 (0.12); 236 (0.12); 239 (0.06)	55	AJ277258
BC335474 (CIT-HSPC 482H14)	CA	83	139 (0.13); 141 (0.17); 143 (0.37); 145 (0.13); 147 (0.18); 149 (0.02)	53	AJ277261
R31646 (LLNL-R 278E6)	GA	37	109 (0.04); 129 (0.11); 131 (0.07); 135 (0.69); 137 (0.09)	55	AJ277259
R31646 (LLNL-R 278E6)	TAA	48	96 (0.76); 99 (0.24)	60	AJ277260
R34169b (LLNL-R 304G9)	CA	79	154 (0.18); 156 (0.02); 158 (0.32); 160 (0.09); 162 (0.23); 164 (0.13); 166 (0.02)	60	AJ277257
R34296b (LLNL-R 306B4)	CA	41	177 (0.57); 179 (0.4); 181 (0.03)	63	AJ277256
R30676 (LLNL-R 268D8)	TTTA	39	166 (0.04); 170 (0.33); 174 (0.54); 178 (0.09)	63	AJ277255

^aHeterozygosity is calculated from allele frequencies observed in a panel of 50 unrelated individuals.

Thus, the dense marker map that we generated provides an efficient framework for refined mapping of disease genes on chromosome band 19p13.3.

All the new markers were examined in the family and two-point lod scores were computed at each locus. A maximum two-point lod score of 2.99 (at $\Theta = 0$) was obtained with the (TAAA) repeat on 34169 cosmid (Table 2). Haplotypes were derived for all subjects, and a recombination event was observed in patient IV-4 (Figure 1b). This crossover narrowed the disease-critical region to the 250 Kb interval between the (TAA) repeat on 31646 cosmid and D19S177 marker.

The 19p13.3 chromosome band contains two putative candidates, the Receptor Type Protein-Tyrosine Phosphatase

Sigma (PTPRS) gene and the GENX3587 transcript. PTPRS (OMIM601576) is a surface glycoprotein that has been implicated in the development of the nervous system. In fact PTPRS is expressed in neuronal tissues in a developmentally regulated fashion.⁴ The *Drosophila* homologue of PTPRS is expressed in CNS axon and implicated in axon pathfinding and motoneuron guidance.⁵ Finally in mice, gene targeting inactivation of PTPRS causes severe neurologic defects including spastic movements, tremor, ataxia gait, abnormal limb flexion and defective proprioception.⁵ GENX-3587 is a muscle-specific transcript that has been mapped within the disease-locus critical region by Pietù *et al*,⁶ we also hypothesised its involvement in the disease pathogenesis. Although

Table 2 Two-point lod score data generated by markers on 19p13.3

Marker	Recombination fraction lod score						
	0.0	0.01	0.05	0.1	0.2	0.3	0.4
27139 (TG)	-0.11	-0.10	-0.06	-0.04	-0.02	-0.01	-0.03
26529 (TA)	-6.5	-2.37	-1.03	-0.51	-0.1	-0.01	-0.04
30140 (GT)	1.67	1.64	1.49	1.31	0.934	0.564	0.24
28154 (ATT)	-1.34	0.40	0.93	1.02	0.88	0.6	0.28
335474 (CA)	-0.35	0.46	0.94	1.02	0.88	0.60	0.28
31646a (GA)	0.96	0.94	0.84	0.71	0.46	0.23	0.06
31646b (TAA)	-0.89	-0.13	0.37	0.50	0.47	0.32	0.14
34169 (TAAA)	2.99	2.93	2.71	2.40	1.78	1.12	0.46
34296 (CA)	1.44	1.41	1.29	1.12	0.80	0.46	0.15
30676 (TTTA)	1.44	1.41	1.29	1.12	0.80	0.46	0.15

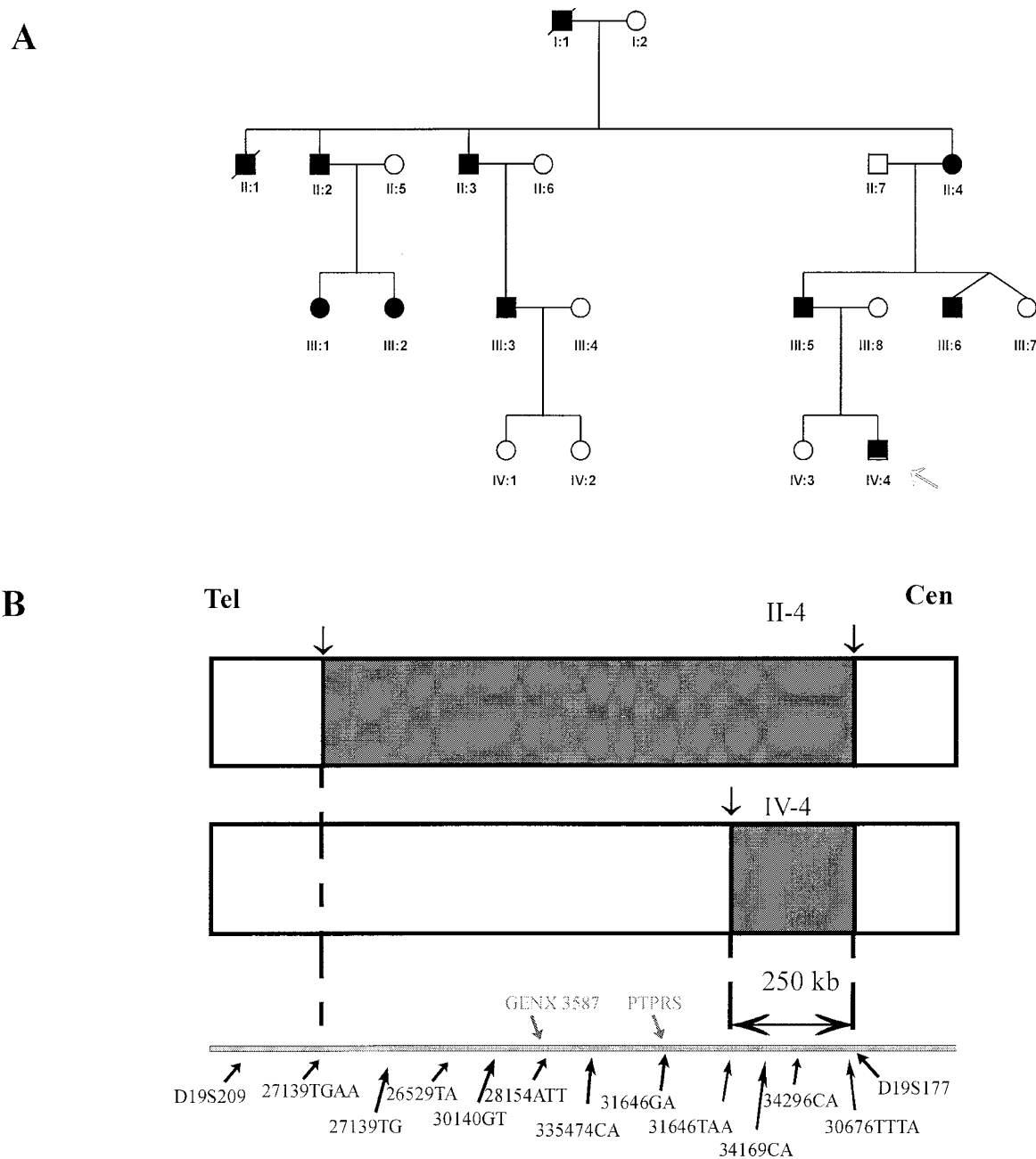


Figure 1 **A** Pedigree of the autosomal dominant vacuola neuromyopathy family. Filled symbols: affected; empty: healthy; slash: deceased. The key recombinant IV-4 individual is indicated by an arrow **B** Schematic genetic map showing the localisation of the markers characterised in this study and the position of GENX387 and PTPRS genes. Crossover between II-4 and IV-4 family member is indicated by a vertical arrow (□).

attractive candidates, both PTPRS and GENX-3587 are ruled out by the crossover event detected in patient IV-4. In fact, the BLAST search tool (available at <http://www.ncbi.nlm.nih.gov/BLAST>) assigned PTPRS and GENX-3587 gene sequences to cosmids R31646 and R28154, respectively, both lying outside the 250 Kb disease interval (Figure 1b). It is

noteworthy that the critical region contains two IMAGE ESTs (clone IMAGE2240016 and IMAGE75431), mapping to cosmid R34296 and R34169, respectively. Elucidating the expression pattern of this transcript in adult and foetal tissues will be essential to determine whether this gene may be involved in the disease pathogenesis.

Acknowledgements

This work was supported by the Italian Telethon (grant no. 1076).

References

- 1 Servidei S, Capon F, Spinazzola A *et al*: A distinctive autosomal dominant vacuolar neuromyopathy linked to 19p13. *Neurology* 1999; **53**: 830–837.
- 2 Lathrop GM, Lalouel JM, Julier C, Ott J: Strategies for multilocus linkage analysis in humans. *Proc Natl Acad Sci USA* 1984; **81**: 3443–3446.
- 3 Kong A, Cox NJ: Allele-sharing models: LOD scores and accurate linkage tests. *Am J Hum Genet* 1997; **61**: 1179–1188.
- 4 Wagner J, Gordon LA, Heng HHQ, Tremblay ML, Olsen AS: Physical mapping of Receptor Type Protein Tyrosine Phosphatase Sigma (PTPRS) to human chromosome 19p13.3. *Genomics* 1996; **38**: 76–78.
- 5 Wallace MJ, Batt J, Fladd CA, Henderson JT, Skarnes W, Rotin D: Neuronal defects and posterior pituitary hypoplasia in mice lacking the receptor tyrosine phosphatase PTP-sigma. *Nat Genet* 1999; **21**: 334–338.
- 6 Pietù G, Eveno E, Soury-Segurens B *et al*: The Genexpress IMAGE knowledge base of the human muscle transcriptome: a resource of structural, functional, and positional candidate genes for muscle physiology and pathologies. *Genome Res* 1999; **9**: 1313–1320.